# Accuracy of Wave Runup Formula on Contrasting Southeast Australian Beaches

**Hannah E. Power[1*], Alexander L. Atkinson[1], Tim Hammond[2] and Tom E. Baldock[2]**
[1] School of Geosciences, University of Sydney, Sydney, Australia; hannah.power@sydney.edu.au
[2] School of Civil Engineering, University of Queensland, Brisbane, Australia
* Current address: Geoscience Australia, GPO Box 378, Canberra ACT 2601, Australia

**Abstract**
This paper presents runup data collected on three contrasting beaches in southeastern Australia. Runup data in this study were collected using optical remote sensing methods. Data were collected at three beaches on the New South Wales and southeast Queensland coastlines. All data are referenced to the Australian Height Datum, which provides a vital reference for local hazard analysis. Data have been analysed to find exceedence statistics for each beach: both the 2% runup exceedence and the maximum runup. These observed values are compared to modelled values from a range of widely used empirical models to assess which model is the most accurate for each beach.

*Keywords: wave runup, swash, empirical models, storms, coastal inundation*

## 1. Introduction

A significant research effort in the coastal zone has been focused on modelling maximum wave runup. This is frequently performed to inform coastal planning and, as such, many researchers aim to produce models that use readily available or easily measureable parameters. These frequently include offshore wave height ($H_o$), wave period ($T$), wavelength ($L$), and beach slope ($\tan\beta$). Maximum runup is of interest to coastal planners as it is used to identify regions at risk from coastal inundation and is also used for planning the locations of future infrastructure. However, the most extreme runup is typically difficult to measure robustly as conditions are frequently such that wave runup impacts or overtops dunes or dune scarps. Consequently, most work focuses on the maximum runup on beaches where the runup is not truncated.

Maximum runup is normally parameterised using either: (1) the maximum runup ($R_{max}$) which is the highest elevation above the still water line (SWL) reached by a single swash event during a given time period, e.g., 15-minutes, and/or (2) the 2% runup exceedence point ($R_{2\%}$) which is the elevation above SWL exceeded by only 2% of swash events during a given time period, e.g., 15-minutes.

Many models used to predict runup have been developed using laboratory data and may therefore have limitations when applied to natural beaches. Others have been developed using data from a single beach or a small number of natural beaches and so may not be applicable on a wide range of natural beaches. Additionally, many of the models were developed using data from North American beaches and while they may be accurate for those particular conditions, wave conditions and bathymetry vary globally and, as a result, the general applicability of these models on Australian beaches is currently unknown. As such, this paper aims to assess the accuracy of a range of models that predict runup for East Australian beaches.

The models tested in this paper are described in Section 2. Section 3 outlines the methods used to collect the Australian field data and the data processing and analysis techniques. Results are presented in Section 4 and the models that are most accurate for each beach are identified. Final conclusions are outlined in Section 6.

## 2. Existing runup models

This study assesses the accuracy of a range of models derived from both laboratory and field data. Each of these models is outlined below. It should be noted that the list of models tested in this paper is not exhaustive.

### 2.1 Models derived from laboratory data

Wassing [12] examined runup in a wave flume with an impermeable structural slope to obtain a parameterisation for $R_{2\%}$:

$$R_{2\%} = 8 \tan\beta \, H_{sig} \qquad (1)$$

where $H_{sig}$ is the significant wave height. Hunt [5] examined maximum runup for monochromatic laboratory waves and found:

$$R_{max} = \xi H_{sig} \qquad (2)$$

where $\xi$ is the Iribarren number. This equation was found to be valid for $\xi \leq 2$. Mase [6,7] investigated random waves on a plain, impermeable slope to find:

$$R = a H_o \xi^b \qquad (3)$$

where $a$ = 1.86 and $b$ = 0.71 for $R_{2\%}$ and $a$ = 2.32 and $b$ = 0.77 for $R_{max}$. van der Meer and Stam [11] examined runup on both smooth and rocky slopes and found:

$$R_{2\%} = C_p \xi_p H_{sig} \quad (4)$$

where $C_p$ varies with swell type and $\xi_p$ is the Iribarren number calculated with the peak period ($T_p$).

### 2.2 Models derived from field data

Douglass [3] used field data from Duck, N.C., U.S.A., and found:

$$R_{max} = H_{m0} \frac{0.12}{\sqrt{{H_{m0}}/{L_o}}} \quad (5)$$

where $H_{m0} = 2\sqrt{2m_0}$, $m_0$ is the variance of the water surface elevation over a one-hour time period, and $L_o$ is the offshore wavelength (m). Stockdon *et al*. [10] used field data from five beaches and developed two models:

$$R_{2\%} = 1.1\left(0.35\beta_f (H_o L_o)^{0.5} + \cdots \frac{\left[H_o L_o \left(0.563\beta_f{}^2 + 0.004\right)\right]^{0.5}}{2}\right) \quad (6)$$

for $\xi_o > 0.3$ where $\tan\beta_f$ is defined as the foreshore slope, and

$$R_{2\%} = 0.043 (H_o L_o)^{0.5} \quad (7)$$

for $\xi_o < 0.3$, with $H_o$ taken as the significant wave height. Nielsen and Hanslow [8] used field data from New South Wales to show:

$$R_{2\%} = 1.98 L_R + Z_{100\%} \quad (8)$$

where $Z_{100\%}$ is the highest vertical level passed by all swash events and:

$$L_R = 0.6 \tan\beta_{FN} \sqrt{H_{orms} L_o} \quad (9)$$

for $\tan\beta > 0.1$ where $\tan\beta_{FN}$ is the beach slope between SWL and $R_{max}$, $H_{orms}$ is the offshore root-mean-square wave height, and:

$$L_R = 0.06 \sqrt{H_{orms} L_o} \quad (10)$$

for $\tan\beta < 0.1$. It should be noted, that the method used by Nielsen and Hanslow to collect data varies significantly from the other studies mentioned here (see [2] for further details). Further, the model contains an additional free parameter $Z_{100\%}$ in comparison to most models, which also needs to be estimated for predictive purposes. $L_R$ has the same functional form as Hunt's formula.

## 3. Methods

### 3.1 Study sites

This study utilises timestacks derived from video data collected from three different beaches over eight days (Figure 1 and Table 1). Data from each day did not cover more than one individual tidal cycle (i.e., 12 h or less). The data were collected from a range of beach types from low tide terrace to longshore bar and trough (Figure 2, Table 1) [14]. All beaches examined in this study are characterised by microtidal, swell dominated conditions, and are located on the east coast of Australia. One and two days of data were collected from South Boganger Beach (SBB) and Norries Head Beach (NHB) respectively (Figure 1). These two beaches lie either side of Norries Head in Cabarita, northern New South Wales (NSW). Five days of data were collected from Main Beach (MB) on North Stradbroke Island, Queensland (Figure 1).

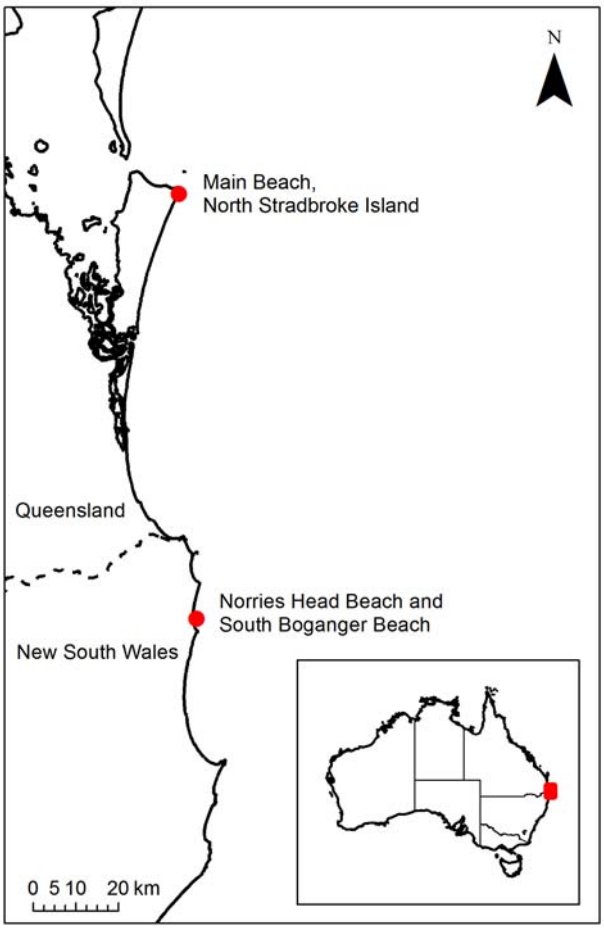


Figure 1 Map showing the location of the three field sites in northern New South Wales and Queensland.

### 3.2 Data collection and pre-processing

Runup data in this study were collected using optical remote sensing methods [1] by placing a portable digital video camera on a headland, foredune, or berm, and focusing on the swash zone. The real world coordinates of a cross-shore line within the field of view were determined by surveying markers placed in the swash zone. Using these data, timestacks were created by sampling frames from the video data at 5 Hz. Pixel intensity profiles were taken along a cross-shore profile from each image and stacked through time to make a timestack (e.g., Figure 3). For further details on this method see [9]. All timestacks were

Table 1 Location, date, number of 15-minute timestacks analysed ($n$), root-mean-square offshore wave height ($H_{orms}$), peak offshore wave period ($T_p$), significant offshore wave period ($T_{sig}$), zero-crossing offshore wave period ($T_z$), beach slope (tan$\beta$), surf scaling parameter ($\varepsilon_b$), and Iribarren number ($\xi_o$) for each day of data used in this study.

| Location | Date | $n$ | $H_{orms}$ (m) | $T_p$ (s) | $T_{sig}$ (s) | $T_z$ (s) | tan$\beta$ (-) | $\varepsilon_b$ (-) | $\xi_o$ (-) |
|---|---|---|---|---|---|---|---|---|---|
| SBB | 09/11/10 | 21 | 1.45 | 7.27 | 6.60 | 5.21 | 0.08 | 11.11 | 0.55 |
| NHB | 10/11/10 | 21 | 1.56 | 8.10 | 7.18 | 5.74 | 0.09 | 8.29 | 0.65 |
| NHB | 11/11/10 | 22 | 1.48 | 8.97 | 7.89 | 6.27 | 0.08 | 7.82 | 0.65 |
| MB | 23/02/11 | 20 | 1.66 | 8.85 | 7.10 | 5.65 | 0.06 | 20.49 | 0.41 |
| MB | 27/02/11 | 22 | 0.85 | 11.05 | 7.78 | 5.76 | 0.03 | 24.61 | 0.32 |
| MB | 28/02/11 | 15 | 0.66 | 9.53 | 6.24 | 5.75 | 0.03 | 37.86 | 0.29 |
| MB | 05/03/11 | 25 | 1.32 | 9.15 | 6.56 | 5.17 | 0.05 | 25.48 | 0.36 |
| MB | 06/03/11 | 25 | 2.04 | 9.02 | 7.28 | 5.80 | 0.06 | 21.52 | 0.38 |

subdivided into 15-minute segments to ensure stationarity with respect to the tide [4].

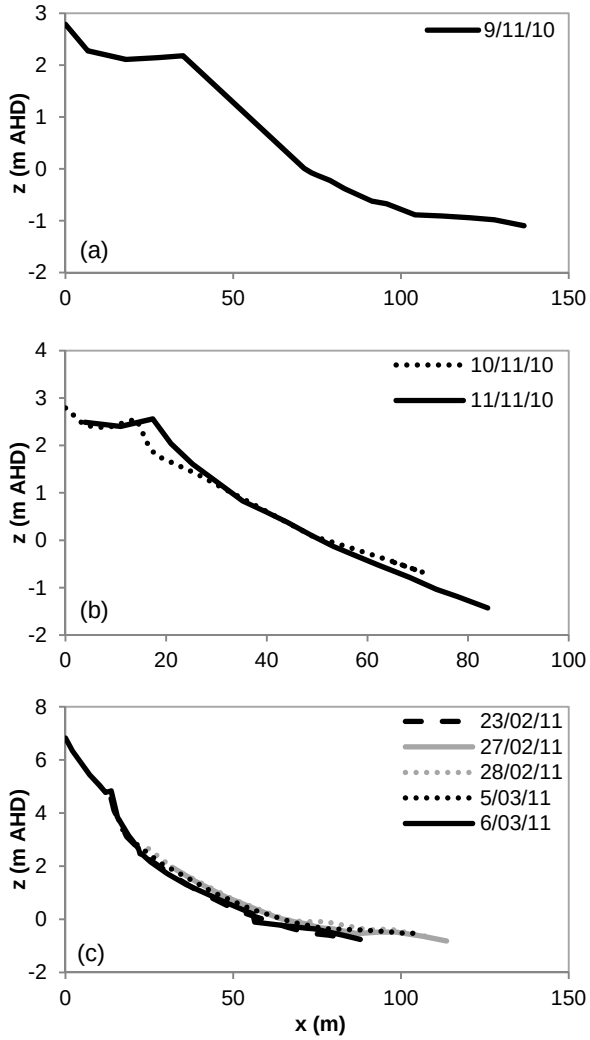


Figure 2 Representative cross-shore beach profiles for each beach on each day of data collection: (a) South Boganger Beach, NSW, (b) Norries Head Beach, NSW, and (c) Main Beach, North Stradbroke Island, Queensland.

Hourly offshore wave and tide conditions were obtained for each measurement day. Data for SBB and NHB were obtained from the offshore waverider buoy at Byron Bay (~40 km south of both beaches in a depth of ~71 m), and data for MB were obtained from the directional waverider buoy located at the Gold Coast (~60 km south of MB in a depth of ~20 m). Cross-shore beach profiles were obtained for each day of data using a total station to survey along the cross-shore profile line used for video data processing. All survey data were reduced to Australian Height Datum using local state and permanent benchmarks.

### 3.3 Extraction of runup data

All timestacks were analysed in Matlab. For each swash event the maximum uprush point was picked manually (Figure 3). Only individual runup events forced by bores were analyzed. It should be noted that not every swash event could be included in the analysis as some swash events were overrun before reaching their maximum uprush point and these were therefore excluded from the analysis. Once each swash event was identified on a given timestack, the x-y pixel locations of the selected points were converted to real-world coordinates using the survey data, and values of vertical excursion for each swash event relative to SWL were calculated.

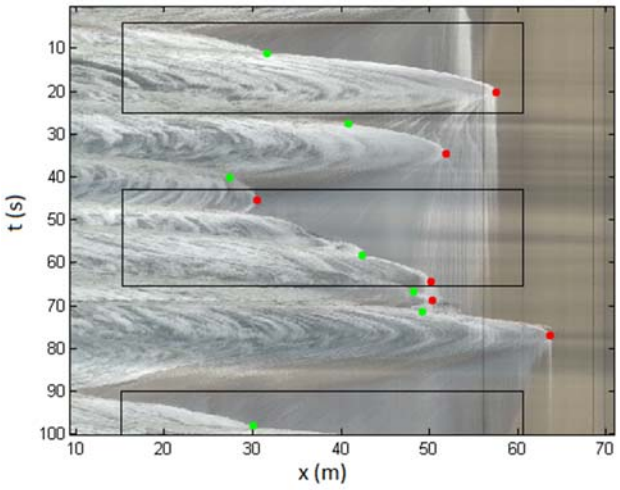


Figure 3 Timestack showing point selection with start- and maximum-uprush points selected (green and red respectively). The black boxes highlight events where one swash overtakes the previous one before flow reversal has occurred.

For each 15-minute timestack, values of $R_{max}$ and $R_{2\%}$ were obtained. $R_{max}$ is defined here as the swash event in a given 15-minute timestack with the greatest vertical excursion relative to SWL. $R_{2\%}$ was calculated using the log-ranking method described in [8]. It should be noted that this assumes the runup distribution is Rayleigh distributed. As such, any 15-minute timestacks that had runup distributions that did not conform to a Rayleigh distribution were not included in the final analysis. An example is shown in Figure 4.

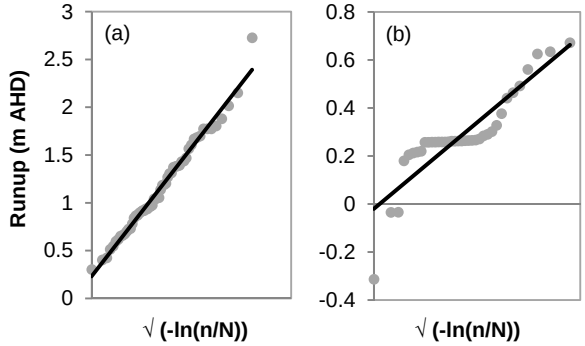


Figure 4 Example log-ranked plots of runup distributions from two 15-minute timestacks where (a) $R^2 \approx 0.98$ (accepted), and (b) $R^2 \approx 0.8$ (rejected).

### 3.4 Assessment of model accuracy

Using the models outlined in Section 2, predicted values of both $R_{2\%}$ and $R_{max}$ were calculated and compared to observed values. In all cases, beach slope was calculated as per the recommendations of each model. For each 15-minute timestack, the model that had the closest predicted value to the observed value for both $R_{2\%}$ and $R_{max}$ was identified as the most accurate model for that timestack. These were then tallied for each beach to identify the most appropriate model for both $R_{2\%}$ and $R_{max}$ for each beach.

It should be noted that in a number of empirical models, it is unclear how wavelength is calculated, i.e., which value of wave period was used. Therefore, the three most commonly available measures of wave period were used to calculate wavelength for model comparisons: zero-crossing period, peak period, and significant period ($T_z$, $T_p$, and $T_{sig}$ respectively), thus resulting in three wavelength values: $L_z$, $L_p$, and $L_{sig}$ and, therefore, three estimates of runup from some models. This was done using:

$$L_o = gT^2/2\pi \qquad (11)$$

where $g$ is the gravitational acceleration ($m.s^{-1}$).

## 4. Results

A total of 3,059 individual run events were obtained from 40 separate 15-minute timestacks at NHB; a total of 1,678 individual runup events were obtained from 21 separate 15-minute timestacks from SBB; and a total of 6,583 runup events were obtained from 110 15-minute timestacks from MB.

Histograms of the most accurate model for each 15-minute timestack are shown for $R_{max}$ and $R_{2\%}$ in Figure 5 and Figure 6 respectively. Data are shown for all timestacks and are also shown for rising tide and falling tide only.

It is clear from Figure 5 that there are differences between model accuracy for $R_{max}$ for each of the three beaches examined here. The Hunt model was most accurate on NHB, with the model being most accurate when using $L_z$ on a rising tide and $L_p$ on a falling tide. The Douglass model was most accurate on SBB overall but was equally as accurate as the Hunt $L_{sig}$ and Hunt $L_z$ models on a rising tide. The Mase model was most accurate on MB with the use of $L_p$ on a rising tide and $L_{sig}$ on a falling tide. It is of interest to note that the Mase model was only the most accurate for MB, never for NHB or SBB, and the Hunt model was only the most accurate for MB for one 15-minute timestack.

In contrast to the clear trends observed for $R_{max}$, the trends of model accuracy for $R_{2\%}$ are not as clear (Figure 6). The Nielsen and Hanslow model using $L_{sig}$ was the most accurate overall on NHB, but on a rising tide the most accurate model was Stockdon *et al*. using $L_z$. On a falling tide, however, the Nielsen and Hanslow model using $L_{sig}$ and the Stockdon *et al*. model also using $L_{sig}$ were equally accurate. On SBB, the most accurate model was the Nielsen and Hanslow model using $L_{sig}$, closely followed by the Nielsen and Hanslow model using $L_p$, with former the most accurate on a rising tide and the latter the most accurate on a falling tide. On MB, the most accurate model was the Mase model using $L_p$, followed by the Nielsen and Hanslow model using $L_p$, with Nielsen and Hanslow's model the most accurate on a rising tide and the Mase model the most accurate on a falling tide. As with the accuracy of the $R_{max}$ models, the Mase model was never the most accurate model for NHB or SBB. Additionally, the Stockdon *et al*. model was only found to be accurate for NHB, never for SBB or MB. The only model that was accurate for all three beaches was the Nielsen and Hanslow model, however, it should be noted that this model requires the additional measured parameter $Z_{100\%}$, over and above offshore wave parameters and beach slope which may increase its predictive skill. In this respect, $Z_{100\%}$ is expected to be related to wave setup, which is implicitly included in the other models.

An example of the range of the predictions for the typical conditions in this study is shown in Figure 7. There is at least a factor 2 difference in the predicted maxima, which is much greater than the variability of the measured 15-minute averaged maxima. The choice of wavelength in the Hunt model yields similar variation to that induced by the

15-minute sampling interval. It is also noteworthy that the largest runup occurs after high tide, and this is also the case for $R_{2\%}$ (not shown). Weir *et al*. [13] identified a similar phenomenon at Avoca Beach (NSW), but no rigorous explanation is available to the authors' knowledge.

In terms of model-data discrepancy, the use of daily averaged wave conditions may lead to some inaccuracy, as changes in wave height over the day were not accounted for.

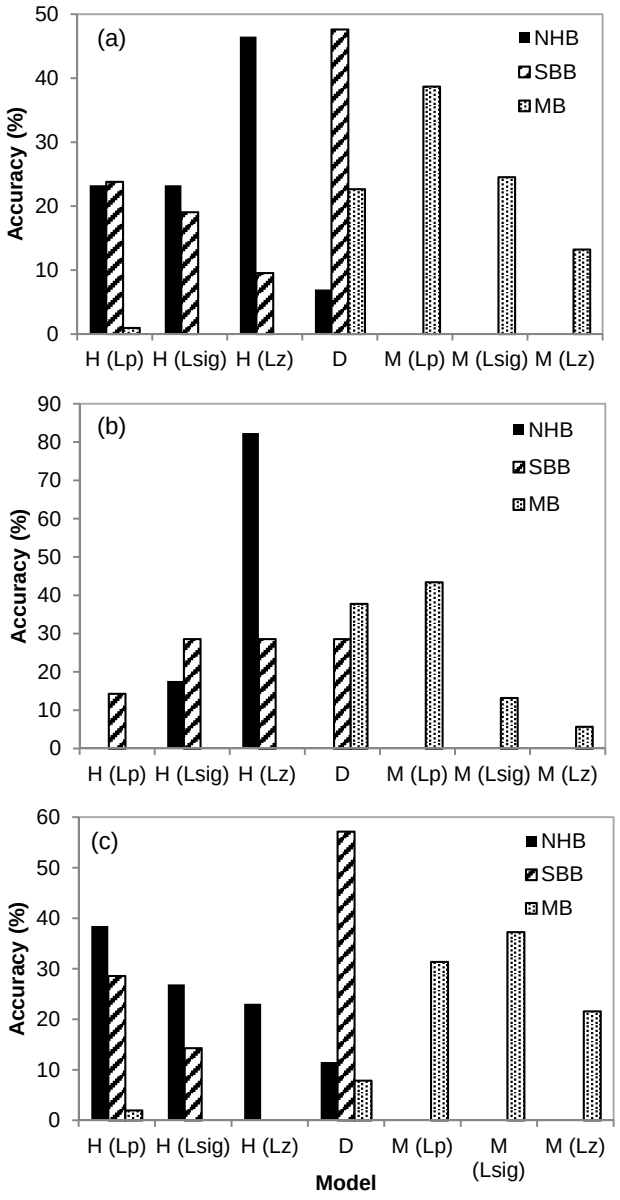


Figure 5 Histograms showing the frequency with each model was found to be the most accurate predictor of $R_{max}$ as a percentage of the total number of 15-minute timestacks collected on each beach for (a) all timestacks, (b) timestacks collected on a rising tide, and (c) timestacks collected on a falling tide. The models tested are as follows: Hunt (H) [5] using $L_p$, $L_{sig}$, and $L_z$, Douglass (D) [3], and Mase (M) [6,7] using $L_p$, $L_{sig}$, and $L_z$.

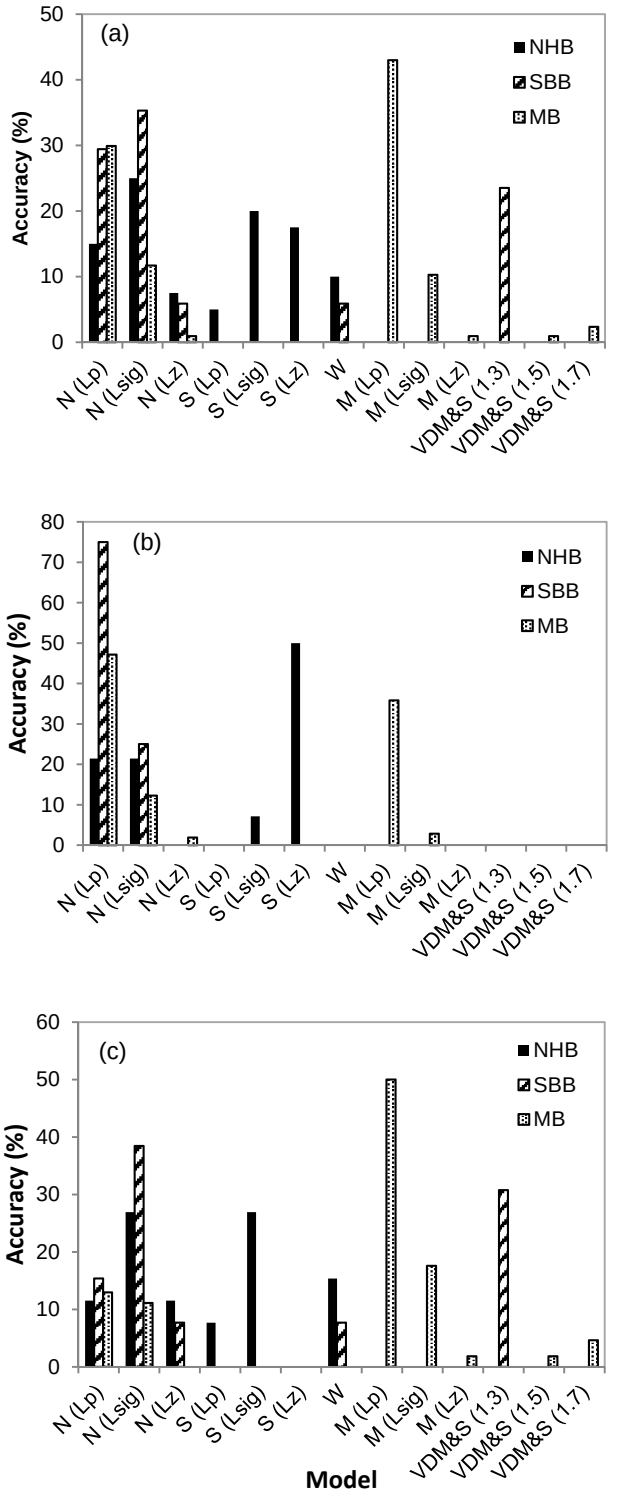


Figure 6 Histograms showing the frequency with each model was found to be the most accurate predictor of $R_{2\%}$ as a percentage of the total number of 15-minute timestacks collected on each beach for (a) all timestacks, (b) timestacks collected on a rising tide, and (c) timestacks collected on a falling tide. The models tested are as follows: Nielsen and Hanslow (N) [8] using $L_p$, $L_{sig}$, and $L_z$, Stockdon *et al*. (S) [10] using $L_p$, $L_{sig}$, and $L_z$, Wassing [12], Mase [6,7] using $L_p$, $L_{sig}$, and $L_z$, and van der Meer and Stam [11] using $C_p$ = 1.3, $C_p$ = 1.5, and $C_p$ = 1.7.

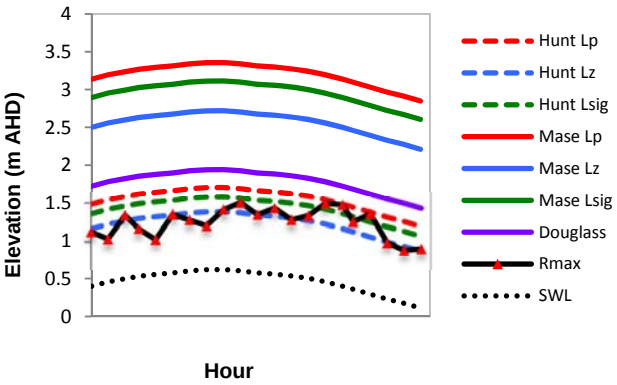


Figure 7 Measured and predicted $R_{max}$ over a single high tide at NHB on 10/11/10.

Model-data discrepancies may also be attributed to due to differences in spectral width and choice of wave period. In a very narrow banded spectrum, the difference between $T_p$ and $T_z$ is minimal, and there is no difference at all for monochromatic waves. At NHB and SBB, the average difference between $T_p$ and $T_z$ (2.53 s) was less than at NS (3.89 s) indicating a more narrow banded spectrum at the Cabarita beaches. Therefore, the models of Mase and van der Meer and Stam may have performed better for more broad-banded spectra and Hunt and Wassing may have performed better in narrow band spectra. Nielsen and Hanslow's model provided some accurate results at all beaches so may be more resilient to differences in wave spectra width. However, $Z_{100\%}$ is a free parameter and the accuracy required for accurate runup predictions is unknown. The influence of different spectral widths on wave runup is not something that has been specifically mentioned in any of the papers reviewed here; therefore, more research may be required to confirm the importance of this variable. Further work is in progress to analyse data obtained over a broader range of beaches. This will be presented at the conference.

## 5. Conclusions

Considering historic climatic data and the current forecasts regarding climate change and sea level rise, the development of a new extreme runup model in which more confidence can be placed will be essential for risk mitigation in eastern Australia. On the basis of this work, however, it is suggested that:

1. For $R_{2\%}$, Mase's model should be used with $L_p$ on more gently sloped beaches ($\tan\beta \leq 0.06$) and Nielsen and Hanslow's model should be used with $L_{sig}$ on beaches where $\tan\beta > 0.06$.
2. For $R_{max}$, Mase's model should be used with $L_p$ on beaches towards the dissipative end of the spectrum ($\tan\beta \leq 0.06$) and Hunt's model be used with $L_p$ or $L_z$ on beaches where $\tan\beta > 0.06$.


## 6. Acknowledgements

Thanks to Ana Vila-Concejo for constructive comments on the thesis by A. L. Atkinson on which this paper is largely based. Thanks to Manly Hydraulics Laboratory within the NSW Department of Public Works and the Queensland Department of Environment and Heritage Protection for offshore wave data. Thanks to the National Tidal Centre at the Bureau of Meteorology for the tidal information. Thanks to the NSW Department of Lands and Planning and the Queensland Department of Environment and Resource Management for data on permanent benchmarks.


## 7. References


[1] Aagaard, T. and Holm, J., (1989), Digitization of wave runup using video records: Journal of Coastal Research, 5, pp. 547–551.

[2] Atkinson, A.L. (2012). Extreme wave runup in eastern Australia: An assessment of existing empirical models, MSc Thesis, University of Sydney, Australia (unpublished), 64 pp.

[3] Douglass, S. (1992), Estimating Extreme Values of Runup on Beaches: Journal of Waterway, Port, Coastal and Ocean Engineering, 118, pp. 220–224.

[4] Hughes, M.G. and Moseley, A.S. (2007), Hydrokinematic regions within the swash zone: Continental Shelf Research, 27, pp. 2000–2013.

[5] Hunt, I.A. (1958), Design of seawalls and breakwaters, U.S. Lake Survey.

[6] Mase, H. (1988), Spectral characteristics of random wave runup: Coastal Engineering, 12, pp. 175–189.

[7] Mase, H. (1989), Random Wave Runup Height on Gentle Slope: Journal of Waterway, Port, Coastal, and Ocean Engineering, 115, pp. 649–661.

[8] Nielsen, P., and Hanslow, D.J. (1991), Wave Run-up Distributions on Natural Beaches, Journal of Coastal Research, 7(4), pp. 1139-1152.

[9] Power, H.E., Holman, R.A. and Baldock, T.E. (2011), Swash zone boundary conditions derived from optical remote sensing of swash zone flow patterns: Journal of Geophysical Research:Oceans, 116, C06007.

[10] Stockdon, H.F., Holman, R.A., Howd, P.A. and Sallenger JR, A.H. (2006), Empirical parameterization of setup, swash, and runup: Coastal Engineering, 53, pp. 573–588.

[11] van der Meer, J.W. and Stam, C.-J.M. (1992), Wave runup on smooth and rock slopes of coastal structures: Journal of Waterway, Port, Coastal, and Ocean Engineering, 118, pp. 534–550.

[12] Wassing, F. (1957), Model investigation on wave runup carried out in the Netherlands during the past twenty years. Proceedings of the 6th International Coastal Engineering Conference, American Society of Civil Engineers, pp. 700–714.

[13] Weir, F.M., Hughes, M.G. and Baldock, T.E. (2006), Beach face and berm morphodynamics fronting a coastal lagoon: Geomorphology, 82, pp. 331–346.

[14] Wright, L.D. and Short, A.D. (1984). Morphodynamic variability of surf zones and beaches: a synthesis: Marine Geology, 56, pp. 93–118.